

Influence of Data Patterns on Reader Performance at Off-Track Reading

Zhejie Liu, Zhimin Yuan, Chun-Lian Ong, and Shiming Ang

Data Storage Institute, Agency for Science, Technology and Research, Singapore 117608

In this paper, we focus our attention on the performance of read heads under the off-track reading condition when the reader is under the influence of the recorded magnetization patterns on the medium, and analyze how the magnetic field due to various data patterns impacts the read head behavior. The analysis is based on the micromagnetic modeling of the state of magnetization in read sensor considering its external magnetic fields due to both the hard bias and the media magnetization pattern. The effects of various magnetization patterns on media are analyzed. The effect of thermal magnetic agitation of the gyromagnetic precession of magnetizations is also evaluated. It is shown that to account for such effect is important for evaluation of magnetic recording schemes for extremely high density.

Index Terms—Finite element analysis, magnetic recording, magnetic sensors, micromagnetics.

I. INTRODUCTION

AS THE bit aspect ratio of the recording tracks reduces in some of the advanced magnetic recording schemes, such as shingled magnetic recording (SMR) and 2-D magnetic recording (2-DMR) [1], an improved understanding of the off-track reading performance of read heads is of interest. Read sensors exhibit various noise sources due to electrical and magnetic origins. Extensive research efforts have been made in the past to gain insight into the various noise mechanism [2]–[6]. The past efforts primarily aim to find out how far the read sensor size can be reduced, and were carried out mostly at the sensor element level. In this paper, we focus our attention on the performance of tunneling magnetoresistance (TMR) read heads at the off-track reading condition when the reader is under the influence of the recorded magnetization patterns on the medium, and attempt to analyze how the magnetic field due to various data patterns impacts the read head behavior. The analysis is based on the micromagnetic modeling of the state of magnetization in read sensor considering of its external magnetic fields due to both the hard bias and the media magnetization pattern. The effects of various magnetization patterns on media are analyzed, including the patterns of neighboring transitions and oppositely polarized neighboring tracks. The results show that at off-track reading the effect of the magnetic field of data patterns on the reader performance can be remarkably significant and accounting for such effect is important for evaluation of the 2-DMR schemes.

II. ANALYSIS OF EXTERNAL FIELDS TO READ SENSOR

Fig. 1 shows a schematic view of a read sensor sweeping over a magnetization pattern of neighboring tracks. One of the reader shields is not drawn in the figure to show the details of the components in the reader. The TMR read sensor has hard bias on both sides, and the stack of the sensor components are placed in between two shields that are not shown in the

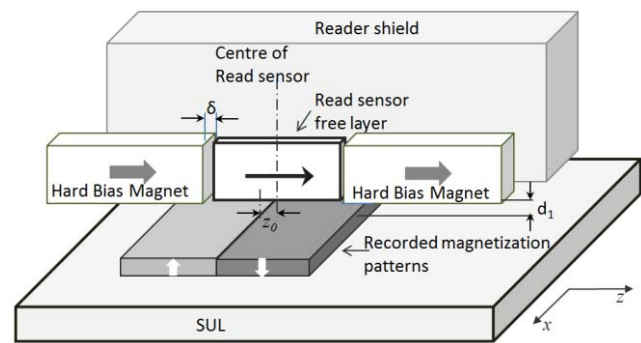


Fig. 1. Schematic view of read sensor over recorded magnetization patterns on media.

figure. The head media combination shown in this figure is used to analyze and to understand the reader performance at off-track reading. In this situation, the read sensor experiences external fields due to the hard bias magnets as well as the magnetization patterns recorded on media. In this section, we first analyzed the external magnetic field applied to the read sensor that plays a critical role in static and dynamic state of the magnetization in the read sensor.

In the analyzes, the parameters of the reader and media are as follows. The free layer of the read sensor has a width of 40 nm, a height of 30 nm, and a thickness of 3 nm, with saturation magnetization of 800 kA/m, exchange coupling constant of 1.0×10^{-11} J/m, and anisotropy field of 7.5 kA/m. The shield to shield spacing is 23 nm. The saturation magnetization of the granular medium, M_s is 500 kA/m. The track width is 65 nm. The head to media spacing is 6 nm. The magnetic field due to the magnetization pattern and the hard bias is analyzed using a finite element method solving the governing Maxwell equations.

Two particular cases are studied; the differences are in the polarizations of the neighboring tracks in relation to the polarization of the hard bias. In the first case, when looking to the direction of the hard bias, i.e., the positive z -direction, the

Manuscript received March 8, 2014; revised May 25, 2014; accepted June 2, 2014. Date of current version November 18, 2014. Corresponding author: Z. J. Liu (e-mail: dsiliuzj@dsi.a-star.edu.sg).

Color versions of one or more of the figures in this paper are available online at <http://ieeexplore.ieee.org>.

Digital Object Identifier 10.1109/TMAG.2014.2329813

0018-9464 © 2014 IEEE. Translations and content mining are permitted for academic research only. Personal use is also permitted, but republication/redistribution requires IEEE permission. See http://www.ieee.org/publications_standards/publications/rights/index.html for more information.

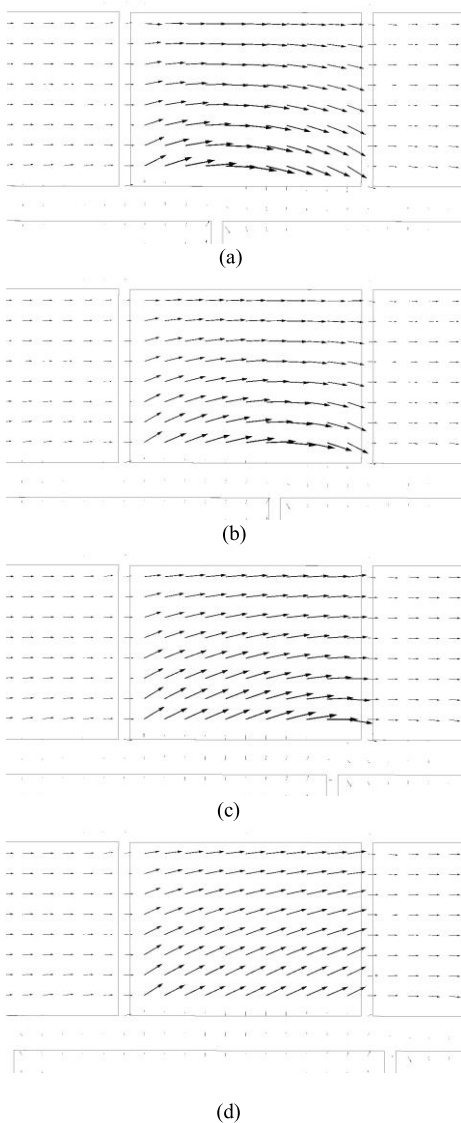


Fig. 2. External magnetic field due to hard bias and media magnetizations in Case 1. The distance between read sensor center and track transition center, z_0 , varies from -5 to 25 nm. (a) $z_0 = -5$ nm. (b) $z_0 = 5$ nm. (c) $z_0 = 15$ nm. (d) $z_0 = 25$ nm.

magnetic polarization of the neighboring tracks points upward, and then downward after the track transition. The magnetic flux vector distributions inside the read sensor element are shown in Fig. 2(a)–(d) corresponding to different read sensor positions relative to the neighboring transitions, measured by the distance between the center of read sensor and the center of the track transition, z_0 , as shown in Fig. 1. It can be seen that the sensor element experienced noticeable variations of the external field in addition to its bias field. Consequently, the reader resistance is affected.

In the second case, the reader is placed over a track edge where the magnetic polarization points downward, and then changed to upward after the track transition when looking in the direction of the hard bias. It can be seen in Fig. 3, that in this case the distribution of the magnetic field due to the hard bias and the media magnetizations is very different from that in Case 1. The variation in the direction and amplitudes of the

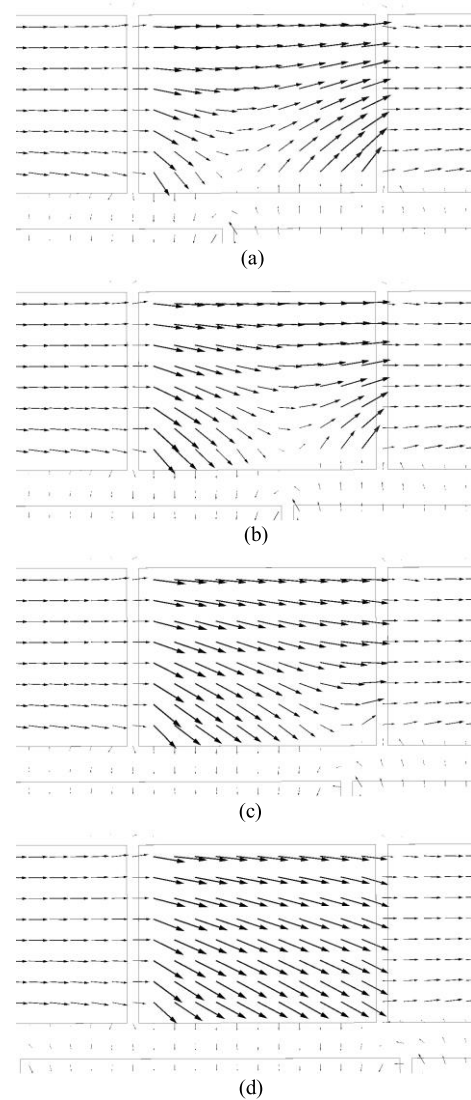


Fig. 3. External magnetic field due to hard bias and media magnetizations in Case 2. The distance between read sensor center and track transition center, z_0 , varies from -5 to 25 nm. (a) $z_0 = -5$ nm. (b) $z_0 = 5$ nm. (c) $z_0 = 15$ nm. (d) $z_0 = 25$ nm.

local magnetic field in the sensor element indicates that the characteristics of the read sensor can be markedly influenced by the magnetization patterns on media.

III. ANALYSIS OF READ SENSOR PERFORMANCE AT OFF-TRACK READING

The reader resistance can be calculated based on the state of magnetization inside the read sensor element obtained using micromagnetic analysis [2], [3], considering the external field due to hard bias and media magnetization. As a coherent movement of the magnetization in the read sensor is no longer assumed, the read sensor can be discretized into smaller geometric elements to obtain the magnetization distribution locally, as shown in Fig. 4. Then the local conductance of each cell of the read sensor can be found accounting for the effect of noncoherent rotation of the local magnetic moment

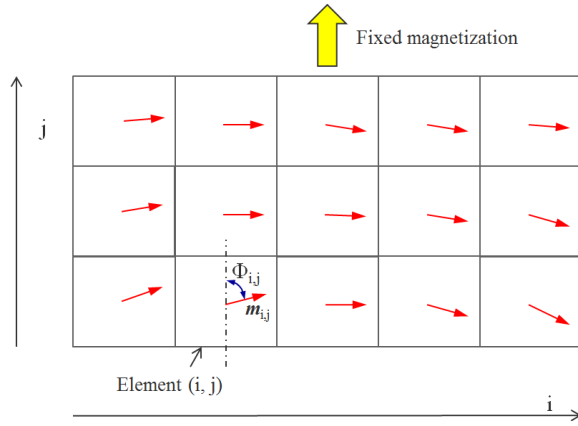


Fig. 4. Schematic view of cells of TMR sensor with noncoherent rotation of magnetic moments under influence of external field due to recorded data.

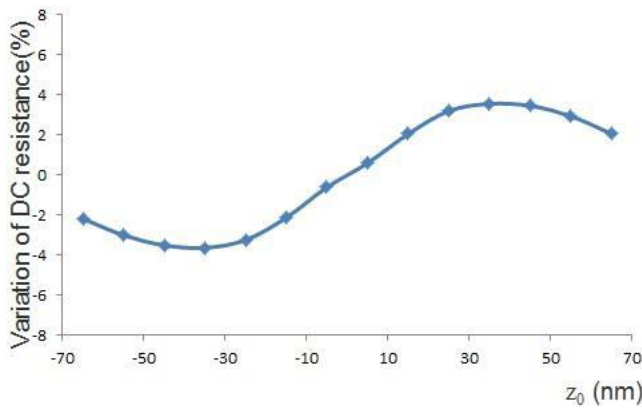


Fig. 5. Variation of reader resistance against read sensor position for Case 1.

as follows:

$$g_{ij} = g_{oij} / (1 + \delta_{oij} \cos \Phi_{i,j}) \quad (1)$$

where $\Phi_{i,j}$ is the angle between the local magnetization, m_{ij} and the vertical axis, as shown in Fig. 4, $\delta_{oij} = \Delta r / (r_{\max} + r_{\min})$, $\Delta r = (r_{\max} - r_{\min})$, $g_{oij} = 1/r_{oij}$, $r_{oij} = (r_{\max} + r_{\min})/2$, and r_{\max} and r_{\min} are the maximum and minimum resistances of the read sensor, respectively.

The total reader conductance can then be obtained using such a discretized model given by

$$G = \sum_i \sum_j (g_{oij} / (1 + \delta_{oij} \cos \Phi_{i,j})). \quad (2)$$

Figs. 5 and 6 show the variation of the reader resistance against the read sensor positions for Case 1 and Case 2, respectively. The variation of the sensor dc resistance is obtained by finding the equilibrium of the time averaged magnetic states in each cell using micromagnetic analysis. It can be observed that peak value of the resistance variation for Case 2 is relatively larger than that for Case 1. In Fig. 7, the analysis of the changes in reader resistance is given when the reader passes a transition in the down-track direction. The curve with triangles gives the reader resistance variation when the reader sweeps over a down-track transition, and then reaches the condition

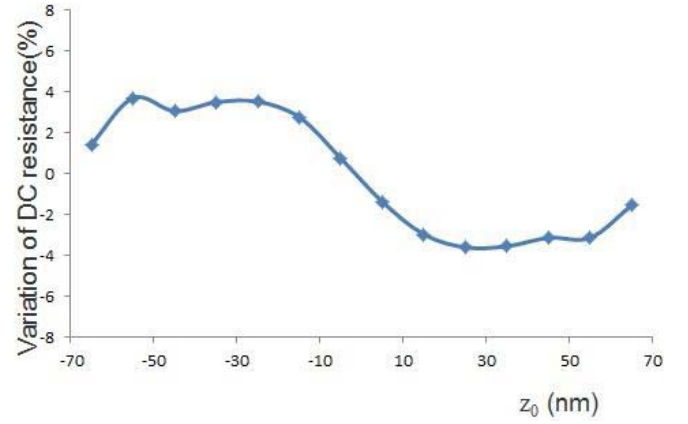


Fig. 6. Variation of reader resistance against read sensor position for Case 2.

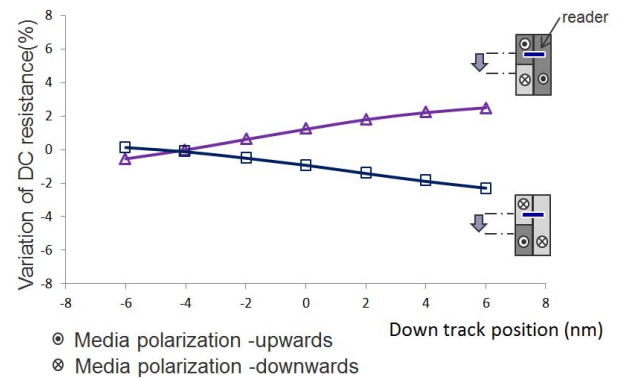


Fig. 7. Variations of reader resistance as read sensor sweeps over a down-track transition with $x = 0$ being the transition center. The squares represent the results for Case 1 and triangles for Case 2.

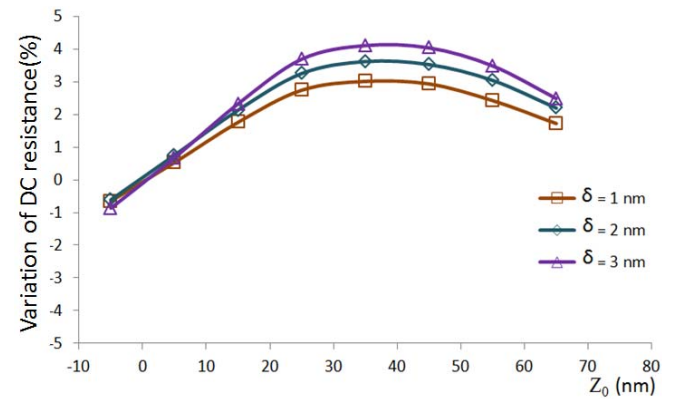


Fig. 8. Variation of reader resistance at different abutting spacing, δ .

of magnetization pattern similar to Case 2. The curve with squares gives the reader resistance variation when the reader moves in the down-track directions and enters the situation of Case 1. It shows that the reader resistance changes depending on the conditions of the recorded magnetization patterns on the media.

The magnetic field external to the read sensor is dependent on various head media parameters. Fig. 8 shows the variation of the reader resistance at different abutting spacing of the hard

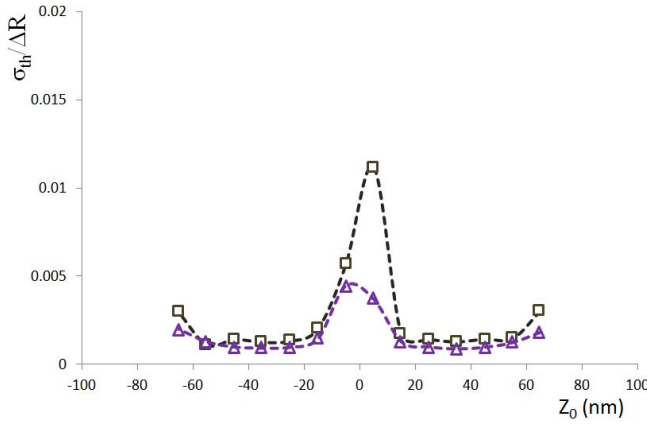


Fig. 9. Thermal magnetic noise at different cross-track positions. (Triangles are results for Case 1 and squares for Case 2.)

bias and the free layer, when the magnetization polarization of the neighboring tracks is arranged as in Case 1. It can be seen that there is a high level of sensitivity to this parameter. It will be noted that such variation is also sensitive to the head and media spacing.

The noncoherence of the local magnetization inside the read sensor due to the media magnetization patterns can also affect its response to the high-frequency variations of the magnetic field and its performance associated with other noise conditions, such as the low-frequency thermal magnetic fluctuation noise [2], [5].

The effect of the thermal agitation of the gyromagnetical precession of magnetizations can be estimated by considering the angular magnetic noise [2]. The rms value of such noise is given by

$$\frac{1}{H_{\text{stiff}}} \sqrt{\frac{2\alpha kT}{\gamma V_c \mu_o M_s \Delta t}} \quad (3)$$

where α is the damping constant ($\alpha = 0.02$), k the Boltzmann constant ($k = 1.38 \times 10^{-23}$ J/k), T the absolute temperature ($T = 300$ K), γ the gyromagnetic ratio ($\gamma = 2.21 \times 10^{-23}$ m/As), M_s the saturation magnetization of the free layer, μ_o the permeability of free space, V_c the volume of the cell element used in the micromagnetic calculations, and Δt is a time constant ($\Delta t = 10$ ps). It is assumed that in Δt the random thermal fluctuation field is of a normal distribution with zero mean and a constant standard deviation [3]. The stiffness field, H_{stiff} , can be calculated as the projection of the effective field onto the direction of the local magnetization in each individual cell element [5].

The rms value of the thermal magnetic noise, σ_{th} , is calculated, and the ratio of σ_{th} over the change in the mean value of the sensor resistance due to the field of the recorded magnetizations on media, ΔR , is plotted against the cross-track positions in Fig. 9. It can be seen that the thermal magnetic noise becomes relatively larger when compared with the sensor signal around the track transition for both Case 1 and Case 2. However, in Case 2 the longitudinal component of the magnetic field due to the recorded magnetizations on media is in general in the opposite direction of the hard bias field, leading to greater degree of stiffness field weakening as compared with that in Case 1. As a result the magnitude of the thermal noise for Case 2 is comparatively larger than that for Case 1, as shown in the figure.

IV. CONCLUSION

In this paper, the performance of hard biased read sensor at off-track reading has been studied. Here, we have focused on the influence of the media magnetic field on the dc resistance, and the thermal magnetic noise of the sensor. A model is introduced for calculation of reader resistance to account for effect of noncoherent rotation of the local magnetic moment. It is effective for studying the reader performance at off-track reading. The effect may need to be properly accounted for in the recording schemes, such as SMR and 2-DMR, especially when the medium with higher coercivity is used and the head to media spacing becomes extremely small.

REFERENCES

- [1] R. Wood, M. Williams, A. Kavcic, and J. Miles, "The feasibility of magnetic recording at 10 terabits per square inch on conventional media," *IEEE Trans. Magn.*, vol. 45, no. 2, pp. 917–923, Feb. 2009.
- [2] J. C. L. van Peppen and K. B. Klaassen, "A new approach to micromagnetic simulation of thermal magnetic fluctuation noise in magnetoresistive read sensors," *IEEE Trans. Magn.*, vol. 42, no. 1, pp. 56–69, Jan. 2006.
- [3] J. Masuko, H. Akimoto, M. Matsumoto, H. Kanai, and Y. Uehara, "Amplitude and phase distributions of magnetization in tunneling magnetoresistive heads," *IEEE Trans. Magn.*, vol. 44, no. 7, pp. 1856–1860, Jul. 2008.
- [4] C. Yoshida, Y. M. Lee, T. Ochiai, Y. Uehara, and T. Sugii, "Micromagnetic study of current-pulse-induced magnetization switching in magnetic tunnel junctions with antiferromagnetically and ferromagnetically coupled synthetic free layers," *Appl. Phys. Lett.*, vol. 99, no. 22, p. 222505, 2011.
- [5] K. B. Klaassen, X. Xing, and J. C. L. van Peppen, "Broad-band noise spectroscopy of giant magnetoresistive read heads," *IEEE Trans. Magn.*, vol. 41, no. 7, pp. 2307–2317, Jul. 2007.
- [6] G. C. Han, B. Y. Zong, P. Luo, and C. C. Wang, "Magnetic field dependence of low frequency noise in tunnel magnetoresistance heads," *J. Appl. Phys.*, vol. 107, no. 9, p. 09C706, 2010.